Biochemical Pharmacology, Vol. 53, 1087–1097, 1997.

ELSEVIER

ISSN 0006-2952/97/$17.00 + 0.00
PII S0006-2952(96)00816-7

Metabolism of the Vitamin D Analog EB 1089: Identification of *In Vivo* and *In Vitro* Liver Metabolites and Their Biological Activities*

Anne-Marie Kissmeyer,†‖ Ernst Binderup,† Lise Binderup,†
Christina Mørk Hansen,† Niels Rastrup Andersen,† Hugh L. J. Makin,‡
N. J. Schroeder,‡ V. Narayanaswamy Shankar§ and Glenville Jones§

†Research Departments, Leo Pharmaceutical Products Ltd., DK-2750 Ballerup, Denmark;
‡Department of Chemical Pathology, The London Hospital Medical College, London E1 2AD U.K.;
and §Department of Biochemistry, Queen's University, Kingston, Ontario K7L 3N6 Canada

ABSTRACT. 1(S),3(R)-dihydroxy-20(R)-(5′-ethyl-5′-hydroxy-hepta-1′(E),3′(E)-dien-1′-yl)-9,10-secopregna-5(Z),7(E),10(19)-triene (EB 1089) is a novel analog of the vitamin D hormone, calcitriol that has been modified in the side-chain resulting in an increased metabolic stability relative to other side-chain modified analogs (e.g. calcipotriol and 22-oxacalcitriol). To further investigate the metabolism of EB 1089, we set out to study this metabolism both in the rat *in vivo* as well as in the postmitochondrial liver fractions from rat, man, and minipig *in vitro*. The same pattern of metabolism was observed in all biological systems employed, both *in vivo* and *in vitro*, namely 26- and 26a-hydroxylation of EB 1089. The same metabolites were produced using cultured cell systems (Shankar *et al.*, see this issue). All the possible isomers of 26- and 26a-hydroxy EB 1089 were synthesised and these were compared to biologically generated material using HPLC, NMR, and GC-MS techniques. The predominant natural isomer observed *in vitro* and *in vivo* in rats as well as *in vitro* in humans was identified to be (25S),26R-hydroxy EB 1089. The biological activities of the EB 1089 metabolites on cell growth regulation were 10- to 100-fold lower than that of EB 1089. The effects of the metabolites on calcium metabolism *in vivo* were comparable to the effect of EB 1089; however, these effects were reduced for the major metabolite in rat and man and for the isomers of 26a-hydroxy EB 1089. We conclude that EB 1089 is metabolised by a different route of side-chain metabolism than calcitriol and that this may explain its relative metabolic stability in pharmacokinetic experiments *in vivo* compared to that of other vitamin D analogs. BIOCHEM PHARMACOL 53;8:1087–1097, 1997. © 1997 Elsevier Science Inc.

KEY WORDS. EB 1089; vitamin D analog; calcitriol; 1,25-dihydroxyvitamin D_3; vitamin D metabolism; pharmacokinetics

$1,25(OH)_2D_3$,¶ the physiologically active form of vitamin D_3, plays a crucial role in the regulation of calcium homoeostasis [1] and in cell growth regulation [2]. The effects of $1,25(OH)_2D_3$ are believed to be mediated *via* a specific intracellular receptor found in many cells and tissues, and are not confined to those involved in the regulation of calcium metabolism. The receptor belongs to the superfamily of steroid receptors [3]. After binding to $1,25(OH)_2D_3$, the receptor-ligand complex acts as a transcription factor that binds to the vitamin D responsive elements on the genome and regulates the expression of a number of genes involved in calcium homeostasis or in the control of cell growth and differentiation, depending on the target cell. The clinical usefulness of $1,25(OH)_2D_3$ is mainly limited by its effect on calcium metabolism, with risk of inducing hypercalcemia and soft tissue calcifications. Therefore, new vitamin D analogs with strong antiproliferative effects, but with reduced effects on calcium metabolism, are of great interest. EB 1089 (Fig. 1) is a novel synthetic analog [4] with strong antiproliferative effects both *in vitro* and *in vivo* combined with a reduced calcemic activity [5–7]. EB 1089 is now undergoing clinical evaluation in patients with proliferative disorders, such as psoriasis and cancer.

* Portions of these results were presented in abstract form at the Bone & Tooth Society Meeting, Warwick, U.K. (March 27, 1995) and the 4th International ISSX Meeting, Seattle, WA, U.S.A. (August 27–31, 1995). Please note that this is a companion article to "Metabolism of the Vitamin D Analog EB1089 by Cultured Human Cells: Redirection of Hydroxylation Site to Distal Carbons of the Side-Chain," by Shankar, Dilworth, Makin, Schroeder, Trafford, Kissmeyer, Calverley, Binderup, and Jones, which published in *Biochemical Pharmacology*, Vol. 53, No. 6, pp. 783–793.

‖ Corresponding author. Dr. Anne-Marie Kissmeyer, Leo Pharmaceutical Products, DK-2750 Ballerup, Denmark. Tel. +45 44 94 58 88; FAX +45 42 84 58 80.

¶ *Abbreviations:* $1,25(OH)_2D_3$, 1α,25-dihydroxyvitamin D_3; EB 1089, 1(S),3(R)-dihydroxy-20(R)-(5′-ethyl-5′-hydroxy-hepta-1′(E),3′(E)-dien-1′-yl)-9,10-secopregna-5(Z),7(E),10(19)-triene; RP-HPLC, reversed-phase HPLC; SP-HPLC, straight-phase HPLC; T½, half-life; AUC, area under the serum level/time curve.

Received 24 June 1996; accepted 9 September 1996.

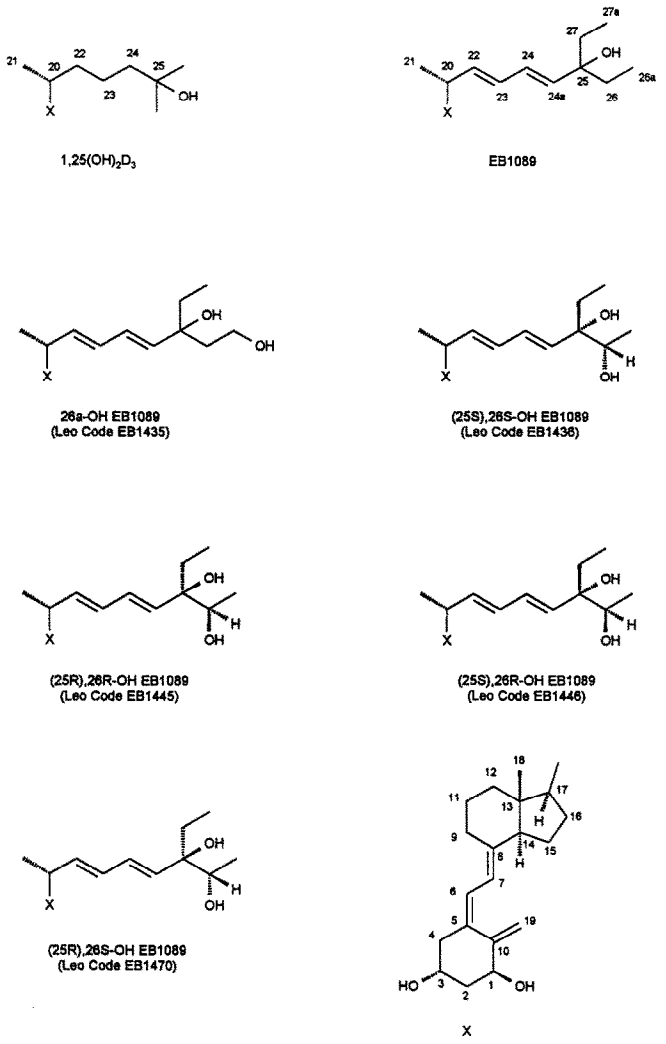

FIG. 1. The chemical structures of $1,25(OH)_2D_3$, EB 1089 and EB 1089 derivatives. X represents the vitamin D ring system.

Pharmacokinetic studies in rats with EB 1089 and $1,25(OH)_2D_3$ have indicated that the metabolic stability of EB 1089 is comparable to that of $1,25(OH)_2D_3$ [8]. This is in contrast to many other synthetic analogs. Calcipotriol and 22-oxa-calcitriol are examples of analogs that are metabolised much faster than $1,25(OH)_2D_3$ [9, 10]. It is likely that the stability of EB 1089 is explained by its side-chain structure, which is different from that of $1,25(OH)_2D_3$ in its featuring 26,27-dimethyl groups, insertion of an extra carbon atom (24a), and 2 double bonds at C_{22} and C_{24}. The hypothesis is that the double bonds block the hydroxylation of C_{23} or $C_{24(24a)}$, which is well known to catabolize $1,25(OH)_2D_3$ [11–13]. Because EB 1089 is a drug designed for systemic administration, it is of importance that it have a certain metabolic stability.

The present paper describes the metabolic stability of EB 1089 *in vivo* in rats and *in vitro* using the postmitochondrial liver fraction (S9) from rats, minipigs, and humans. It also describes the isolation and identification of the major metabolites from *in vitro* systems. Finally, the biological activities of these metabolites are presented.

MATERIALS AND METHODS

Materials

$1,25(OH)_2D_3$, EB 1089, [19-^{14}C]EB 1089, the four diastereoisomeric forms of 26-hydroxy EB 1089, and the two 26a-hydroxy epimers of EB 1089 (Fig. 1) were synthesised at Leo Pharmaceutical Products (Ballerup, Denmark) ([4], synthetic details will be published elsewhere). The absolute configuration at C_{26} of the four 26-hydroxy diastereoisomers is known from the synthetic pathway. The two 26S diastereoisomers (Leo code names: EB 1436 and EB 1470) were synthesised by using one enantiomer of a particular building block, and the optical antipode was used in the preparation of the two 26R diastereoisomers (Leo code names: EB 1445 and EB 1446). The configuration at C_{25} of these four diastereoisomers was not determined but, according to Cram's rule [14], EB 1436 and EB 1446 are 25S compounds and EB 1445 and EB 1470 are 25R compounds. The two 26a-hydroxy epimers (Leo code name: EB 1435) were not separated from each other. All other chemicals and reagents were commercially available.

Animals and Biological Methodology

IN VIVO METABOLISM. The pharmacokinetics of $1,25(OH)_2D_3$ and EB 1089 have previously been described [8]. Briefly, male rats were given a single i.v. dose of 200 μg/kg and blood samples were taken up to 4 hr after dosing. This high dose was chosen as a compromise between a tolerable dose and one that would give measurable serum concentrations of the test compound. For investigation of the metabolic profile, groups of 3 male Sprague Dawley rats were given a single i.v. dose of 30 μg/kg [^{14}C]EB 1089 (138 kBq/kg). The livers and kidneys were taken at 0, 0.5, 2, and 4 hr after administration from different groups of animals each time. The tissues were homogenated in 1 volume of 0.1 M Na-phosphate buffer pH 7.4 and were further prepared as described for serum [8]. Briefly, the homogenates were precipitated with 1 volume of acetonitrile and, after centrifugation, the supernatants were diluted with buffer before being injected into the RP-HPLC system.

IN VITRO METABOLISM. $1,25(OH)_2D_3$ or [^{14}C]EB 1089 was incubated with a liver metabolizing system, containing 100 μL of the postmitochondrial liver fraction (S9) from rats, minipigs, or humans (Human Biologics, Phoenix, AZ) per mL in 8 mM $MgCl_2$, 33 mM KCl, 5 mM glucose-6-phosphate, and 4 mM NADP in 0.1 M phosphate buffer pH 7.4. The final concentration of the test compound was 4×10^{-6} M (2 MBq/μmol EB 1089). The incubations were performed at 37°C, and the samples were collected at 0–4 hr after addition of the test compound. The samples were prepared as previously described for serum [8] before being injected into the RP-HPLC system.

BIOLOGICAL GENERATION OF METABOLITES OF EB 1089 FOR IDENTIFICATION BY COMIGRATION ON HPLC. The native metabolites were generated from the rat S9 metabolizing system (see above) using an incubation time of 2 hr. The samples were prepared for SP-HPLC using a BondElut

LRC C18/OH cartridge (Analytichem International, Harbor City, CA) as described previously [9] and reconstituted in the mobile phase. Identical samples were prepared for RP-HPLC, as described previously [8]. In addition, each of the synthetic 26-hydroxy and 26a-hydroxy derivatives was added (5 μL of 4×10^{-5} M) separately to the reconstituted samples before injection into SP- or RP-HPLC.

Analytical Procedures

HIGH-PERFORMANCE LIQUID CHROMATOGRAPHY. The RP-HPLC analysis was performed as previously described [8], except that a Waters 996 Photodiode Array Detector (Millipore A/S, Hedehusene, Denmark) was coupled in series with a Radiomatic Flo-One/Beta Model A-250 Radioactivity Flow Detector (Radiomatic Instruments & Chemical Co., Meriden, CT) to allow for the simultaneous collection of PDA spectra and radiochromatograms, respectively. The SP-HPLC system consisted of a Spectraphysics SP 8770 isocratic pump (Spectraphysics, San Jose, CA), a Merck-Hitachi L-4200 UV-VIS Detector (E. Merck, Darmstadt, Germany), a Rheodyne 7161 injection valve (Rheodyne Incorporated, Cotati, CA), and a Millennium 2010 Chromatography Manager (Millipore A/S, Hedehusene, Denmark). The analytical column was a Merck Superspher Si 60, 4 μm, 125 × 4 mm column (E. Merck, Darmstadt, Germany). The eluent was hexane-isopropanol-methanol (90:5:5, v/v/v) with a flow-rate of 2 mL/min. The wave length of detection was 264 nm.

NMR AND MASS SPECTROMETRY. The metabolites were generated as above, but microsomes were used instead of a postmitochondrial fraction (S9). Therefore, glucose-6-phosphate dehydrogenase (1 IU/mL) was added, and the concentration of EB 1089 was 2×10^{-5} M. Peaks I, II, and III were separated on RP-HPLC as described above. After evaporation of the RP-HPLC solvent, the residues of the individual peaks (I and II) were redissolved in CD_3CN (Uvasole® Merck) and, after a trace of tetramethylsilane (TMS) was added, used for NMR determination. The concentration of the individual metabolites in the NMR solutions was estimated to be in the range of 1–5 micrograms per 0.6 mL. Blank preparations as well as diluted solutions of pure EB1089 were used as reference to identify impurities originating in the workup procedure. All proton spectra were obtained on a Bruker ARX500 spectrometer (Bruker Analytische Messtechnik, Rheinstetten, Karlsruhe, Germany) equipped with a 5-mm broadband inverse probe and z gradient equipment. A pulse angle of 30° was used together with a pulse repetition time of 1 sec. Up to 15000 transients were collected. An exponential multiplication of 0.2 Hz was applied to the FID before FT. The spectra were recorded at 300° K. Chemical shifts are given in ppm delta scale using TMS as internal reference. The GC-MS procedure for peaks I, II, and III is described in the subsequent paper (Shankar *et al.*, see this issue). Briefly, prior to mass spectrometry, samples were run on SP-HPLC (using a solvent mix hexane-isopropanol-methanol (95:5:5,v/v/v), LiChrospher Si 60, 4 mm i.d. × 125 mm (E. Merck, Darmstadt, Germany), flow 1 mL/min). The eluent was monitored using a photodiode array detection system, and peaks with the characteristic UV spectrum associated with EB 1089 and its metabolites were collected. The solvent was evaporated and trimethylsilylimidazole was added. After incubation for 1 hr at 50°C, the derivatives were purified on hydroxyalkoxypropyl Dextran Type IX (Lipidex 5000) columns (Sigma Chemical Company, Dorset, U.K.) eluting with hexane. GC-MS was carried out as described previously [15].

Biological Assays

EFFECTS ON U 937 CELL PROLIFERATION. U 937 human monocytic tumour cells (American Type Culture Collection, Rockville, MD) were grown in RPMI 1640 supplemented with 10% fetal calf serum (FCS). The cells were incubated in a humidified atmosphere at 37°C in the absence and presence of the test compounds (10^{-12} to 10^{-7} M). After 96 hr of incubation, the cells were counted and the concentration of test compound resulting in 50% inhibition (IC_{50}) of cell proliferation was calculated from the dose-response curve.

EFFECTS ON HaCaT CELL PROLIFERATION. HaCaT human hyperproliferating skin cells (kindly supplied by Dr. N. E. Fusenig, German Cancer Research Center, Heidelberg, Germany) were propagated in Phenol Red-free Dulbecco's modified Eagle's medium supplemented with 5% FCS, 2 mM glutamine, 100 IU/mL penicillin, and 100 μg/mL streptomycin. The cells were incubated in a humidified atmosphere at 37°C in the absence and presence of the test compounds (10^{-11} to 10^{-7} M). After 120 hr of incubation, DNA synthesis was determined by incorporation of ^{3}H-labelled thymidine. Each sample was tested in quadruplicate, and the concentration of test compound resulting in 50% inhibition (IC_{50}) of DNA synthesis was calculated from the dose-response curve.

BINDING TO THE INTESTINAL RECEPTOR FROM RACHITIC CHICKENS. The isolated receptor for $1,25(OH)_2D_3$ from the intestinal epithelium of rachitic chickens was purchased from Amersham (Buckinghamshire, U.K.). 500 μL of receptor protein was incubated with approximately 10,000 dpm [^{3}H]-$1,25(OH)_2D_3$, and increasing concentrations of test compound were added. After incubation for 60 min at 22°C, bound and free [^{3}H]-$1,25(OH)_2D_3$ were separated on dextran-coated charcoal. The samples were centrifuged and the supernatants containing the receptor-bound [^{3}H]-$1,25(OH)_2D_3$ were counted in a liquid scintillation counter. The concentration of the test compound resulting in a 50% displacement of bound [^{3}H]-$1,25(OH)_2D_3$ was calculated.

EFFECTS ON CALCIUM METABOLISM. LEW/MOL female rats (130–170 g) were placed in metabolism cages for 7 days. Test compounds were administered orally each day for 7 days. Control rats received propylene glycol. Each group consisted of 3 rats. Urine was collected daily, and blood was collected by cardiac puncture on day 7. Calcium levels in

TABLE 1. The pharmacokinetics of EB 1089 and $1,25(OH)_2D_3$ in rats, and the metabolic stability of EB 1089 and $1,25(OH)_2D_3$ in the postmitochondrial liver fraction from rats, minipigs, and humans

		*In vivo**			*In vitro**
Compound	**Species**	**T½(β), (hr)**	**AUC∞ (ng/mL × hr)**	**Clearance (mL/hr/kg)**	**T½ (hr†)**
EB 1089	Rat	2.1	255	784	1.3 ± 0.05‡
	Pig	–	–	–	1.6 ± 0.13‡
	Man	–	–	–	1.4 ± 0.09‡
$1,25(OH)_2D_3$	Rat	2.2	7355	27	2.5 ± 0.15§
	Pig	–	–	–	3.0 ± 0.11‖
	Man	–	–	–	2.4 ± 0.59‖

* See also [8]; †mean ± SD; ‡n = 3, §n = 7; ‖n = 2.

urine and serum were determined by complex formation with o-cresolphthalein, using a Hitachi 705 autoanalyzer (Boehringer Manheim, Kvistgaard, Denmark). The urinary excretion of calcium was calculated from days 3–7 (steady-state conditions) and expressed in mmol/day (mean ± SD). Serum calcium was measured on day 7 and expressed in mmol/L (mean ± SD). Statistical analysis was carried out using Student's *t*-test.

RESULTS

Metabolism Studies In Vivo *and* In Vitro

Table 1 shows the pharmacokinetic parameters of EB 1089 and $1,25(OH)_2D_3$ *in vivo* and *in vitro*. The T½ of EB 1089 in rats is equivalent to the half-life of $1,25(OH)_2D_3$. On the other hand, the AUC_∞, which indicates the concentration and persistence of a drug in the serum, is much higher for $1,25(OH)_2D_3$ than for EB 1089, due to the lower binding affinity of EB 1089 to DBP compared to $1,25(OH)_2D_3$ [8]. Moreover, the serum clearance, the volume of serum cleared totally from the drug per time unit, varies inversely with the AUC_∞; thus, the clearance of EB 1089 is much faster than that of $1,25(OH)_2D_3$. However, when [^{14}C]EB 1089 was administered to rats, we found that the analog was concentrated in the liver. Thus, the concentration of [^{14}C]EB 1089 was *ca.* 50 ng per g and *ca.* 10 ng per mL serum 30 min after administration of 30 μg/kg i.v. In addition, whole body autoradiographic investigations with [^{14}C]EB 1089 revealed that highest concentration of [^{14}C]EB 1089 was found in the liver (data not shown). The liver samples collected at 0.5, 2, and 4 hr after dosing showed all 3 peaks more polar than the parent compound (Fig. 2A–D), with the highest level of metabolites seen at the 2-hr sampling time. A similar metabolic profile was obtained from the analysis of kidney samples, although the concentration of EB 1089 and the metabolites were much lower. Using the postmitochondrial liver fraction (containing the microsomal fraction) obtained from rats, minipigs, and humans, we were able to generate the same 3 peaks as *in vivo* (Fig. 2). These observations indicate that at least a qualitatively identical liver metabolism occurs *in vivo* and *in vitro* in rats, as well as *in vitro* in the 3 species. The 3 peaks were also detected using a PDA detector, and this technique revealed that each peak possessed the same UV absorption spectrum as EB 1089, thereby indicating retention of side-chain unsaturation. Finally, the *in vitro* metabolic stabilities (T½) of EB 1089 in the 3 species were comparable (Table 1), but the T½ of $1,25(OH)_2D_3$ *in vitro* was almost 2-fold that of EB 1089.

Isolation and Identification of the Metabolites

Using the rat liver microsomal preparation, larger quantities of EB 1089 metabolites were generated to identify the metabolites. All of the 4 possible isomers of 26-hydroxy EB 1089, as well as the 2 possible 26a-hydroxy EB 1089 isomers (not separated), were synthesised and their migration both on SP- and RP-HPLC were compared with the biologically generated metabolites. Figure 3A,B shows a sample collected after 2 hr of incubation with EB 1089 run under both HPLC conditions. On RP-HPLC (A), the largest peak was designated I and the minor peaks II and III. Correspondingly, the peaks on SP-HPLC (B) were designated 1, 2, and 3. The relative retention times of these peaks were compared with the retention time of the synthetic EB 1089 derivatives after the separate addition of each to the biological samples (Table 2). Thus, on RP-HPLC, peak I comigrates exclusively with (25S),26R-hydroxy EB 1089 (EB 1446); peak II comigrates with the two 26S isomers of 26-hydroxy EB 1089, as well as with one of the 26a-hydroxy EB 1089 isomers (b); peak III comigrates with the opposite 26a-hydroxy EB 1089 isomer (a) and with (25R),26R-hydroxy EB 1089 (EB 1445). Moreover, on SP-HPLC, peak 1 comigrates with the (25S,26R) and (25R,26S) isomers of 26-hydroxy EB 1089; peak 2 comigrates with the (25S,26S) and (25R,26R) isomers of 26-hydroxy EB 1089; and peak 3 comigrates with 26a-hydroxy EB 1089 (both isomers). To permit an unambiguous identification of all the observed peaks, it was necessary to collect peaks I, II, and III separately from RP-HPLC and reinject them into SP-HPLC. In addition, peaks 1 and 2 were collected from SP-HPLC and reinjected into RP-HPLC. These results are summarised in Table 2, which shows that peak I was, as stated earlier, identical to (25S),26R-hydroxy EB 1089 (EB 1446) which, after 2 hr of incubation, corresponded to *ca.* 20% of the initial concentration of EB 1089. Peak II corresponded to the two 26S isomers of 26-hydroxy EB 1089, each of which

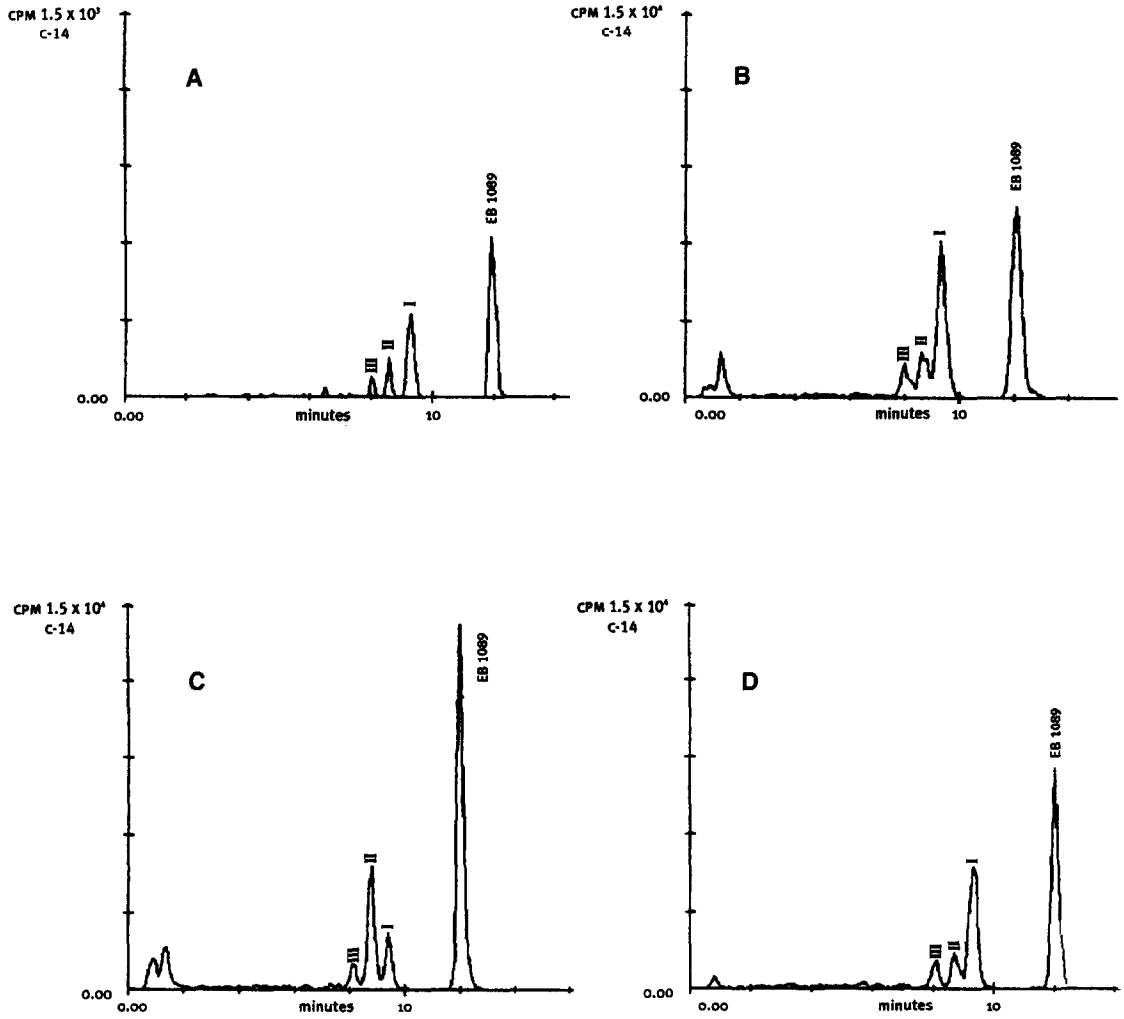

FIG. 2. Radiochromatograms from a liver sample taken 4 hr after i.v. administration of 30 μg/kg [^{14}C]-EB 1089 to rats (A); and from 4-hr incubations of [^{14}C]-EB 1089 with postmitochondrial liver fraction from rats (B), minipigs (C), and humans (D). Metabolites were separated on a LiChrospher 100 RP-18 (5 μm, 125 x 4 mm) column using a linear water-methanol gradient from 70 to 95% methanol over 20 min at a flow rate of 2 mL/min. A Radiomatic Flo-One/Beta model A-250 Radioactivity Flow Detector was used and Pico Aqua was used as scintillator at a flow rate of 4 mL/min.

corresponded to *ca.* 5% of the initial EB 1089 concentration. Peak III corresponded to (25R),26R-hydroxy EB 1089 (EB 1445), with its concentration *ca.* 2% of the initial EB 1089 concentration. In addition, peak III also contained traces of 26a-hydroxy EB 1089 (isomer a).

In addition to the identification of the metabolites by comigration studies on HPLC, peaks I, II, and III (isolated from RP-HPLC) were examined using NMR and GC-MS spectrometry. Peak I: In the proton NMR spectrum of peak I, resonances from the protons in positions 1, 3, 4, 6, 7, 9, 18, and 19 were clearly observed. Compared to EB1089, the chemical shift of these protons is proof of an unchanged structure of ring A, as well as the triene system. An unchanged stereochemistry in positions 13, 14, and 17 was strongly supported, and the spectrum furthermore indicated that substitution did not take place in rings C and D. The double bond protons from the side-chain prove the existence of an all *trans* diene system, as in EB1089. A minor change in the chemical shift of these protons was, nevertheless, observed (Fig. 4A). The most pronounced differences between the proton NMR spectrum of peak I and EB1089 were found in the 0.8 to 1.1 ppm region (Fig. 4B). The intensity of the triplet from the methyl protons in positions 27 and 27a were found to be only half the expected value. This indicates that a reaction took place in one of the ethyl groups (positions 26, 26a, 27, and 27a). In addition, a doublet (three protons) assignable to the methyl in a CH_3CH-O- system was observed at 1.03 ppm. The corresponding CH-O- proton was expected to be observable in the 3.5 ppm region. Due to overlapping lines from solvent impurities in this region, no absolute proof of the existence of such a proton could be given or excluded. From the NMR spectra, peak I could be assigned to an EB1089-like structure with an additional hydroxyl in the 26 position. For example, Fig. 4A and B show part of the NMR spectra of a synthetic (25S),26R-hydroxy EB 1089 (EB 1446), EB 1089, and the biologically generated metabolite, respectively. Peak II: The proton NMR spectrum of peak II

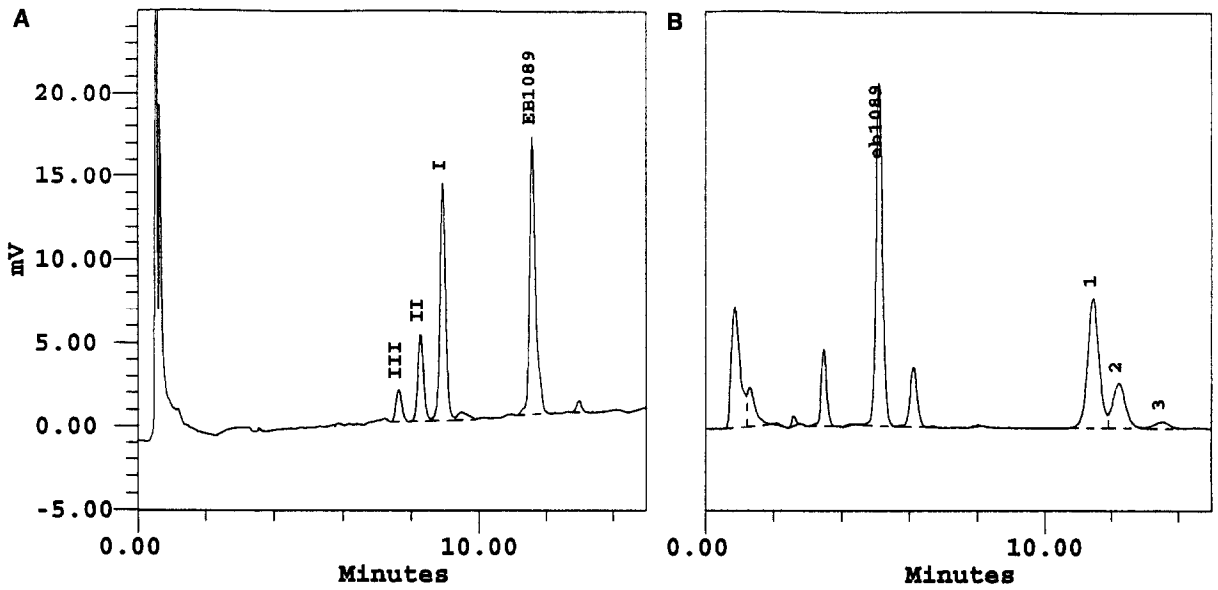

FIG. 3. Reversed-phase (A) and straight-phase (B) chromatograms (UV at 264 nm) from 2-hr incubations of EB 1089 with postmitochondrial liver fraction from rats. (A) Metabolites were separated on a LiChrospher 100 RP-18 (5 μm, 125 × 4 mm) column using a linear water-methanol gradient from 70 to 95% methanol over 20 min at a flow rate of 2 mL/min. (B) Metabolites were separated on a Superspher Si 60 (4 μm, 125 × 4 mm) column using the solvent hexan-isopropanol-methanol (90:5:5) at a flow rate of 2 mL/min. The wave length of detection was 264 nm.

in principle shows the same features as the spectrum of peak I. The samples investigated were more impure than those investigated from peak I, but the spectra supported the structure with an additional hydroxyl in the 26 position. From the given NMR spectra, it was not possible to conclude whether peak II consisted of one or more isomers. Peak III: The quantity of peak III was too small to obtain any reliable proton NMR spectra.

As stated above, the 3 putative metabolites (peaks I, II, and III) could be resolved into multiple compounds on SP- and RP-HPLC, each with an EB 1089-like spectrum. Each peak was derivatised and a mass spectrum of the *pyro*-isomer was obtained. Two distinct types of mass spectra were observed. The fragment m/z 217, which arises by cleavage in the A ring ($TMSiOC_1$-C_2-C_3 TMSi) and is seen in all 1,3 dihydroxylated vitamin D derivatives, was observed in both spectra: Type A (peak I, both compounds from peak II and a major part from peak III); the molecular ion was at m/z 758, indicating that this compound was a monohydroxylated metabolite of EB 1089. The base peak was at m/z 641, representing the ion $(M-117)^+$ derived by cleavage between C_{25} and C_{26} with loss of the C_{26}-OTMSi-$C_{26a'}$. The subsequent loss of silanols from m/z 641 gave m/z 551 and 461. Cleavage between C_{25} and C_{26} also gave rise to an

TABLE 2. Identification of biologically generated (rat liver S9) EB 1089 metabolites by comigration with synthetic standards

Compound	Origin	Relative retention time		Identification of EB 1089 derivatives after reinjection and their amount after 2 hr of incubation (% compared to the initial amount of EB 1089)
		SP-HPLC	RP-HPLC	
EB 1089 (=X)	Synthetic	1	1	
26a-OH-X (a)	Synthetic	2.65	0.660	
26a-OH-X (b)	Synthetic	2.65	0.710	
(25S),26S-OH-X	Synthetic	2.39	0.715	
(25R),26R-OH-X	Synthetic	2.40	0.656	
(25S),26R-OH-X	Synthetic	2.24	0.769	
(25R),26S-OH-X	Synthetic	2.24	0.715	
Peak I	Liver S9	–	0.771	(25S),26R-OH (20%)
Peak II	Liver S9	–	0.715	(25S),26S-OH (5%) + (25R),26S-OH (5%)
Peak III	Liver S9	–	0.659	(25R),26R-OH (2%) + 26a-OH (trace)
Peak 1	Liver S9	2.26	–	(25S),26R-OH (20%) + (25R),26S-OH (5%)
Peak 2	Liver S9	2.41	–	(25S),26S-OH (5%) + (25R),26R-OH (2%)
Peak 3	Liver S9	2.65	–	26a-OH (trace)
Peak A*	HPK1A-*ras* cells	2.40	0.654	(25R),26R-OH
Peak B*	HPK1A-*ras* cells	2.65	0.659	26a-OH

* Metabolites of EB 1089 that have been formed in human keratinocyte HPK1A-*ras* cells as described in the subsequent paper (Shankar *et al*).

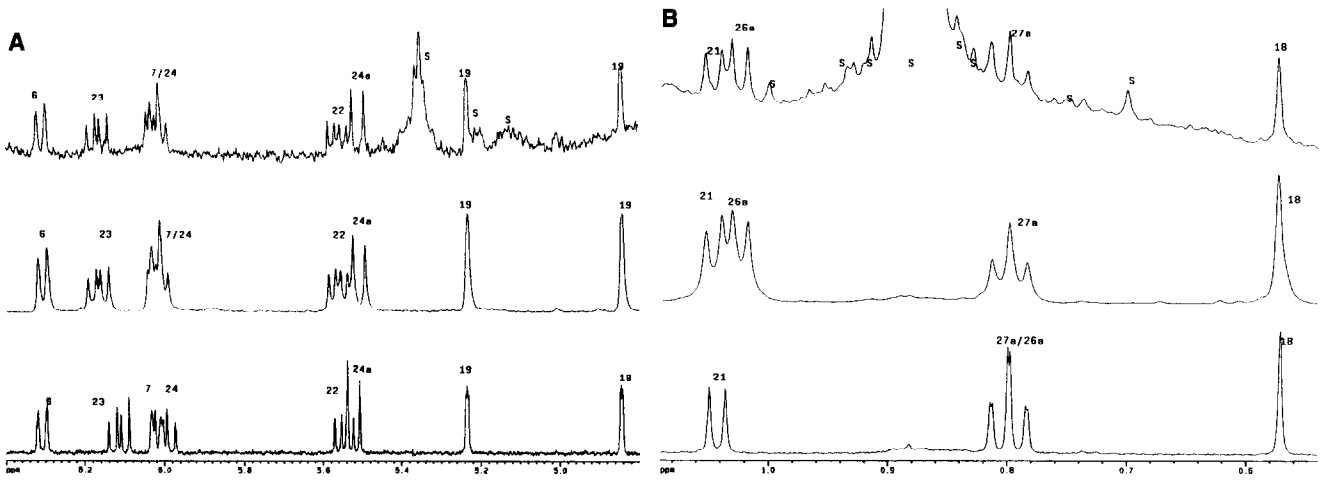

FIG. 4. (A) The ^{1}H-NMR spectrum (region 6.4 to 4.8 ppm) of peak 1 (upper trace), (25S),26R hydroxy EB 1089 (EB 1446) (middle trace) and EB 1089 (lower trace), respectively. Solvent CD_3CN. Reference tetramethylsilane. Assignments are given according to the numbers used in Fig. 1. S designates impurities from the workup procedure. (B) The ^{1}H-NMR spectrum (region 1.09 to 0.54 ppm) of peak I (upper trace), (25S),26R hydroxy EB 1089 (EB 1446) (middle trace) and EB 1089 (lower trace), respectively. Solvent CD_3CN. Reference tetramethylsilane. Assignments are given according to the numbers used in Fig. 1. S designates impurities from the workup procedure.

ion at m/z 117, indicating the presence of vicinal hydroxyls on C_{25} and C_{26} because the charge goes to both fragments in such cases. Other ions were seen at m/z 668 $(M\text{-}90)^+$ and m/z 743 $(M\text{-}15)^+$. An important fragment was also present at m/z 183, which arose by cleavage between C_{23} and C_{24} (m/z 273) and subsequent loss of silanol. This fragmentation is consistent with the structure of 26-hydroxy EB 1089. Type B (minor compound from peak III): The molecular ion of this spectrum was, once again, at m/z 758, indicating as before a monohydroxylated metabolite of EB 1089. The intensity of the molecular ion in type B spectra is usually higher than in type A spectra, although it was not at all seen in the spectrum of IIIc, though its mass/charge ratio could be inferred from the peaks at m/z 627 and 729 $(M\text{-}29)^+$, the 29 amu fragment arising by loss of C_{27}-C_{27a}, m/z 639 $(M\text{-}29\text{-}90)^+$ and m/z 668 $(M\text{-}90)^+$. The base peak was at m/z 627 $(M\text{-}131)^+$. Other fragments were seen at m/z 183, m/z 103 (loss of the C_{26a} silanol) m/z 339 (by cleavage of side-chain between C_{17} and C_{20}) and m/z 249 $(339\text{-}90)^+$. This fragmentation is consistent with a structure of 26a-hydroxy EB 1089. In summary, the GC-MS spectra obtained with peaks I and II were very similar to those obtained with peak A, which was isolated from HPK1A-*ras* cells, as demonstrated in the subsequent paper (Shankar *et al.*, see this issue). Peak A was identified as 26-hydroxy EB 1089. Moreover, one of the compounds in peak III had the same spectrum as that of peak B isolated from the HPK1A-*ras* cells. This peak B was identified as 26a-hydroxy EB 1089.

Biological Activities of the Synthetic Metabolites of EB 1089

The 26-hydroxy and 26a-hydroxy derivatives of EB 1089 were tested *in vitro* in different biological assays and the results are given in Table 3. HaCaT, a spontaneously immortalised nontumorigenic human skin keratinocyte cell line, was used as an *in vitro* system suitable for testing the effects of vitamin D analogs on skin cells [16]. Moreover, U937, a tumorigenic human histiocytic lymphoma cell line, was used as an *in vitro* system suitable for testing the effects of vitamin D analogs on cancer cells [17]. The effects (IC_{50} values) of the metabolites on inhibition of the proliferation of HaCaT and U937 cells were all markedly reduced compared to EB 1089, with the (25R,26S) isomer of 26-hydroxy EB 1089 (EB 1470) the most active compound among the derivatives. The binding affinity for the chicken intestinal vitamin D receptor varied between the derivatives, but they all had a lower affinity for the receptor than did EB 1089. Finally, the effects on calcium metabolism were investigated (Table 4). The effects of the metabolites of the two 25R isomers of 26-hydroxy EB 1089 on calcium metabolism *in vivo* appeared to be slightly higher than that of EB 1089, and the effects of 26a-hydroxy EB 1089 and (25S),26R-hydroxy EB 1089 (EB 1446) were markedly reduced.

DISCUSSION

The objective of the present investigations was to identify the main *in vivo* and *in vitro* metabolites of EB 1089 in various species, as well as to determine their biological activities in calcemia and cell-proliferation assay systems. We focused on hepatic metabolism *in vitro* because a large proportion of EB 1089 is found in the liver quickly after its systemic administration. It has been demonstrated in these studies that EB 1089 is metabolised to 26- and 26a-hydroxy derivatives. The stereospecific identifications are based upon HPLC comigration studies using biologically generated metabolites compared with synthetic derivatives. Sup-

TABLE 3. In vitro activities of EB 1089 and its monohydroxylated derivatives

Compound	Inhibition of proliferation HaCaT IC_{50} (M)(*)	Inhibition of proliferation U937 IC_{50} (M)(*)	Receptor binding 50% displacement of [^{3}H]-1,25$(OH)_2D_3$ (M)(*)
EB 1089 (=X)	7.9×10^{-10} (90)	5.8×10^{-10} (79)	1.7×10^{-10} (0.4)
26a-OH-X	1.0×10^{-7} (0.9)	3.4×10^{-8} (1)	1.1×10^{-9} (0.06)
(25S),26S-OH-X	3.2×10^{-8} (3)	6.3×10^{-9} (7)	1.6×10^{-9} (0.04)
(25R),26R-OH-X	7.1×10^{-8} (1)	5.8×10^{-9} (8)	4.6×10^{-10} (0.14)
(25S),26R-OH-X	1.3×10^{-8} (5)	2.3×10^{-9} (2)	$>3.5 \times 10^{-9}$ (<0.04)
(25R),26S-OH-X	4.0×10^{-9} (16)	4.6×10^{-10} (9)	1.0×10^{-9} (0.2)

* Activity relative to 1,25$(OH)_2D_3$ from the actual experiment, in which the activity of 1,25$(OH)_2D_3$ was set at 1.

portive data were provided by NMR- and mass spectroscopy (GC-MS) of metabolites collected following incubation of EB 1089 with the postmitochondrial liver fraction from rats. Although all definitive identifications were based on metabolites generated *in vitro* from rat liver homogenates, it is very important to note that similar HPLC profiles of the metabolites were obtained from livers of rats dosed with EB 1089. In addition, incubations of EB 1089 with the postmitochondrial liver fraction from rats, minipigs, and humans produced the same metabolic profiles. On the other hand, the relative amount of each metabolite varied depending upon the origin of the sample, which necessitates the development of an HPLC method that could separate all six 26- and 26a-hydroxy EB 1089 isomers simultaneously. Nevertheless, it appears that (25S),26R-hydroxy EB 1089 (EB 1446), which is well separated from all the other isomers, is the most abundant metabolite observed *in vivo* in rats and *in vitro* after incubation of EB 1089 with the postmitochondrial liver fraction from rats and humans. On the other hand, because of technical difficulties, it was not clear which of the 26-hydroxy EB 1089 isomers are the most abundantly generated from the postmitochondrial liver fraction of minipigs. Irrespective of the exact stereochemistry of the 26-hydroxy EB 1089 produced in the various *in vivo* and *in vitro* systems from different species, it is also reassuring to see that hydroxylation occurs at the C_{26} and C_{26a} positions in intact cultured cell *in vitro* models used in the subsequent paper (Shankar *et al.*, see this issue). In this context, it is remarkable that a number of different 26-hydroxy isomers are formed, although it seems that the 26R isomers are the preferred metabolite formed both *in vivo* and in various *in vitro* systems used here and in the subsequent paper (Shankar *et al.*, see this issue). In addition to these metabolites, more polar and minor metabolites have been observed and these are considered to be metabolites further along the biodegradation pathway of EB 1089.

Pharmacokinetic data have demonstrated that the serum half-lives of EB 1089 and 1,25$(OH)_2D_3$ are similar, at least when rats were given equal high doses of each compound and when the half-lives were based on serum concentrations up to 4 hr after dosing. Using much lower doses would have been more pharmacologically and physiologically relevant, but determination of EB 1089 in serum after administration of lower doses presents a number of difficulties. A

TABLE 4. Calcium levels in urine and serum after p.o. administration of EB 1089 and its monohydroxylated derivates

Compound	Dose (μg/kg/day p.o 7×)	Calcium in urine (mmol/day) Mean ± SD		Calcium in serum (mmol/L) Mean ± SD	
None (vehicle)	0	21 ± 13	–	2.76 ± 0.09	–
EB 1089 (×)	0.5	71 ± 27	$P<0.001$	2.88 ± 0.03	n.s.
	1.0	136 ± 39	$P<0.001$	2.86 ± 0.10	n.s.
	2.5	255 ± 75	$P<0.001$	2.98 ± 0.11	n.s.
None (vehicle)	0	23 ± 7	–	2.78 ± 0.10	–
26a-OH-X	1.0	35 ± 12	$P<0.01$	2.76 ± 0.04	n.s.
	10	126 ± 44	$P<0.001$	2.88 ± 0.07	n.s.
(25S),26S-OH-X	1.0	139 ± 45	$P<0.001$	2.91 ± 0.04	n.s.
	10	DEAD	–	DEAD	–
(25R),26R-OH-X	1.0	221 ± 63	$P<0.001$	3.09 ± 0.21	n.s.
	10	DEAD	–	DEAD	–
None (vehicle)	0	17 ± 6	–	2.87 ± 0.08	–
(25S),26R-OH-X	0.5	23 ± 9	$P<0.05$	2.98 ± 0.01	n.s.
	1.0	31 ± 15	$P<0.01$	2.86 ± 0.11	n.s.
	10	149 ± 63	$P<0.001$	3.36 ± 0.23	$P<0.05$
(25R),26S-OH-X	0.5	53 ± 20	$P<0.001$	2.89 ± 0.11	n.s.
	1.0	113 ± 29	$P<0.001$	3.02 ± 0.17	n.s.
	10	DEAD	–	DEAD	–

The effects of EB 1089 and its monohydroxylated derivates on calcium metabolism *in vivo* were determined in 3 separate experiments, each including a control group (vehicle).

sensitive bioassay combined with HPLC is under development but, until the assay is functional, a less sensitive HPLC method with a limit of detection of 10 ng/mL remains in use. Therefore, rats had to be treated with relatively high doses (200 μg/kg) to make it possible to measure EB 1089 up to approximately 4 hr after dosing. However, most of the effects of vitamin D analogs (including regulation of the hydroxylases) are genetically regulated and appear at approximately 24 hr after treatment. Thus, it is questionable whether or not the toxic effects of the compounds appear within the first 4–6 hr after dosing. In any event, no increases in serum calcium could be observed (data not shown). Moreover, the half-lives and other pharmacokinetic parameters that were compared were based on the same dose levels and calculation intervals, with only vitamin D analogs compared. In addition, the serum half-life of EB 1089 has been determined to be 2.5 hr (calculated from 1–6 hr, 5 sampling times, 2–3 rats per time and r = 0.99) in a study where male rats were given a single dose of 30 μg [^{14}C]EB 1089 per kg i.v. (Personal communication, Hanne Sørensen). Although the dose used in that study was more than 10-fold higher than any therapeutically relevant doses, it confirms our results obtained with a much higher dose.

The hypothesis that the conjugated double bonds in the side-chain would protect the molecule from being either 23 or 24/24a hydroxylated seems to have been confirmed, because no signs of the formation of such metabolites have been observed in any of the *in vivo* or *in vitro* systems investigated. The enzymes responsible for the formation of the isomers of 26- and 26a-hydroxy EB 1089 metabolites have not yet been identified. However, in the subsequent paper (Shankar *et al.*, see this issue), it has been demonstrated that ketoconazole can inhibit their formation, indicating that cytochrome P450 enzymes are involved in the biotransformation of EB 1089. On the other hand, Shankar *et al.* also suggested that neither CYP24 nor CYP27 was involved, by using a transfected COS-1 cell system [18]. In the search for identification of the enzymes responsible for the formation of 26- and 26a-hydroxy EB 1089 metabolites, it is notable that 1,25,26-trihydroxy vitamin D_3 can be produced from $1,25(OH)_2D_3$ incubated with kidney homogenates from vitamin D-repleted chickens [19]. The same metabolite has also been identified in plasma from cows given large doses of vitamin D_3 [20]. Very little is known about this minor biodegradation pathway of $1,25(OH)_2D_3$, but it has been demonstrated that 1,25,26-trihydroxy vitamin D_3 is not a precursor for $1,25(OH)_2D_3$ 26,23 lactone, either in intact rats or in nephrectomised rats [21]. Moreover, intestinal 26-hydroxylase activity has been shown to be the same in rats with or without renal failure [22]. Further experiments are needed to investigate whether or not the same 26-hydroxylase is responsible for the formation of 26-hydroxy and/or 26a-hydroxy metabolites of EB 1089. It seems that mammalian 26-hydroxylase is not active in the kidney, which correlates well with our findings that EB 1089 could not be biotransformed using rat kidney homogenate (data not shown). In addition, the concentration of 26-hydroxy metabolites in kidneys obtained from rats dosed with EB 1089 was very low compared to the concentration in the liver. Thus, the presence of metabolites may be due to transportation from the liver and/or to a low activity of 26-hydroxylase in the kidneys. On the other hand, EB 1089 was easily biotransformed in the liver homogenate. Therefore, it is suggested that the first step in the biodegradation of EB 1089 occurs in the liver. This is in contrast to $1,25(OH)_2D_3$, which is metabolised mainly in the intestine and kidney [11–13]. Furthermore, in a comparative study with $1,25(OH)_2D_3$ and EB 1089 in mice, it has been demonstrated that EB 1089 has a 50-fold lower affinity for renal 24-hydroxylase [23]. Taken together, this could explain why $1,25(OH)_2D_3$ was metabolised slower in the liver *in vitro* system than EB 1089 was, although $1,25(OH)_2D_3$ and EB 1089 were metabolised at the same rate *in vivo*. Thus, it is suggested that the main biodegradation pathways for EB 1089 and $1,25(OH)_2D_3$ are not catalysed by the same initial enzymes. In such case, the risk that EB 1089 can have an impact on the physiological levels of $1,25(OH)_2D_3$, is reduced. This hypothesis is supported by the demonstration that pretreatment of rats for 1 week with the maximal tolerated dose of EB 1089 did not influence the pharmacokinetics of $1,25(OH)_2D_3$ (data not shown). The same is also demonstrated in the subsequent paper (Shankar *et al.*, see this issue), where EB 1089 fails to change the rate of catabolism of $1,25(OH)_2D_3$ in HPK1A-*ras* cells. This is in contrast to another synthetic vitamin D analog, 22-oxa-calcitriol, which probably does share the same catabolic enzymes as $1,25(OH)_2D_3$ [24], and has been shown to increase the degradation of $1,25(OH)_2D_3$ [25–26].

The present biological studies with the 26-hydroxy and 26a-hydroxy metabolites of EB 1089 have demonstrated that their biological activities, in general, are lower than that of their parent compound. The lowest activity was observed for 26a-hydroxy EB 1089, which also appeared to be present in the lowest amount. The most abundant metabolite in rats and humans was (25S),26R-hydroxy EB 1089 (EB 1446), which also had a very reduced activity compared to EB 1089. The calcium activity of the 26-hydroxy EB 1089 derivatives was, except for (25S),26R-hydroxy EB 1089 (EB 1446), comparable to that of EB 1089 or somewhat higher. Based upon the activity of the derivatives and the concentration in which they are present, it is suggested that they have only a minor influence on the overall systemic effect of EB 1089. It is, therefore, most likely that the biological effects observed from *in vivo* experiments are related directly to EB 1089, unless an extensive and different metabolism occurs in the target cells. In relation to the biological activities, it is remarkable that the two 25R isomers of 26-hydroxy EB 1089 have a markedly higher affinity for the vitamin D receptor than the two 25S isomers of 26-hydroxy EB 1089. This observation may con-

tribute to the understanding of the ligand conformation in the receptor-ligand complex. In addition, this higher affinity may be related to their relatively strong effects on calcium metabolism *in vivo*. However, a direct correlation between the binding affinity for the vitamin D receptor and the biological activities *in vitro* of the compounds could not be found in the present investigation. This is in agreement with previous studies that have shown that the biological effects of vitamin D compounds are not determined by receptor affinity alone, but also by the ability of the compounds to induce vitamin D-receptor transcription [27].

In summary, the liver is an important organ for the metabolism of EB 1089. The major metabolites observed in the liver after administration of EB 1089 to rats, as well as those observed following incubation of EB 1089 with the post-mitochondrial liver fraction from rats, minipigs, and humans, are 26-hydroxy and 26a-hydroxy isomers of EB 1089. The same metabolites were also formed in intact cultured cell *in vitro* models as described in the subsequent paper (Shankar *et al.*, see this issue). Thus, independently of the identification technique (HPLC, NMR, or GC-MS) and of the models used for generation of the metabolites, the studies demonstrated that 26-hydroxy isomers of EB 1089 were the major metabolites and that 26a-hydroxy EB 1089 was the minor metabolite. This finding is important, especially because the doses of EB 1089 that can be given to humans without the risk of hypercalcemia are so low that it is very difficult to measure the serum levels of either EB 1089 or its metabolites. Therefore, most knowledge of the pharmacokinetics and metabolism of EB 1089 must be based on *in vitro* experiments and studies in other species *in vivo*. Investigations in various target cells are also useful (e.g. the cultured cell *in vitro* models used in the subsequent paper) (Shankar *et al.*, see this issue). At present, the metabolism of EB 1089 is being investigated in various target cells where strong effects on cell growth regulations have been demonstrated.

References

1. DeLuca HF, Krisinger J and Darwish H, The vitamin D system. *Kidney Int* **38:** S2–S8, 1990.
2. Reichel H, Koeffler HP and Norman AW, The role of the vitamin D endocrine system in health and disease. *N Engl J Med* **320:** 980–991, 1989.
3. Haussler MR, Jurutka PW, Hsieh JC, Thompson PD, Selznick SH, Haussler CA and Whitfield GK, New understanding of the molecular mechanism of receptor-mediated genomic actions of the vitamin D hormone. *Bone* **17:** S33–S38, 1995.
4. Binderup E, Calverley M and Binderup L, In: *Vitamin D_3 Gene Regulation, Structure Function Analysis and Clinical Applications, Proceedings on the Eighth Workshop on Vitamin D, Paris, France, 5–10 July 1991* (Eds. Norman AW, Bouillon R and Thomasset M), pp. 192–193. Walter de Gruyter, New York, 1991.
5. Mathiasen IS, Colston KW and Binderup L, EB 1089, a novel vitamin D analogue, has strong antiproliferative and differentiation-inducing effects on cancer cells. *J Steroid Biochem Molec Biol* **46:** 365–371, 1993.
6. Colston KW, Mackay AG, James SY, Binderup L, Chander S and Coombes RC, EB 1089: A new vitamin D analogue that inhibits the growth of breast cancer cells *in vivo* and *in vitro*. *Biochem Pharmacol* **44:** 2273–2280, 1992.
7. Haq M, Kremer R, Goltzman D and Rabbani SA, A vitamin D analogue (EB 1089) inhibits parathyroid hormone-related peptide production and prevents the development of malignancy-associated hypercalcemia *in vivo*. *J Clin Invest* **91:** 2416–2422, 1993.
8. Kissmeyer AM, Mathiasen IS, Latini S and Binderup L, Pharmacokinetic studies of vitamin D analogues: relationship to vitamin binding protein (DBP). *Endocrine* **3:** 263–266, 1995.
9. Kissmeyer AM and Binderup L, Calcipotriol (MC 903): Pharmacokinetics in rats and biological activities of metabolites. *Biochem Pharmacol* **41:** 1601–1606, 1991.
10. Dusso AS, Negrea L, Gunawardhana S, Lopez-Hilker S, Finch J, Mori T, Nishii Y, Slatopolsky E and Brown AJ, On the mechanism for the selective action of vitamin D analogs. *Endocrinology* **128:** 1687–1692, 1991.
11. Mayer E, Bishop JE, Chandraratna RAS, Okamura WH, Kruse JR, Popjak G, Ohnuma N and Norman AW, Isolation and identification of 1,25-dihydroxy-24-oxo-vitamin D_3 and 1,23,25-trihydroxy-24-oxo vitamin D_3. *J Biol Chem* **258:** 13458–13465, 1983.
12. Reddy SG and Tserng K-Y, Calcitroic acid, end product of renal metabolism of 1,25-dihydroxy vitamin D_3 through C-24 oxidation pathway. *Biochemistry* **28:** 1763–1769, 1989.
13. Makin G, Lohnes D, Byford V, Ray R and Jones G, Target cell metabolism of 1,25-dihydroxyvitamin D_3 to calcitroic acid. *Biochem J* **262:** 173–180, 1989.
14. Cram JC and Elhafez FAA, Studies in stereochemistry. X. The rules of steric control of asymmetric induction in the syntheses of acyclic systems. *J Am Chem Soc* **74:** 5828–5834, 1952.
15. Qaw F, Calverley MJ, Schroeder NJ, Trafford DJ, Makin HL and Jones G, *In vivo* metabolism of the vitamin D analog, dihydrotachysterol. Evidence for formation of 1 α,25- and 1 β,25-dihydroxy-dihydrotachysterol metabolites and studies of their biological activity. *J Biol Chem* **268:** 282–92, 1993.
16. Binderup L, Carlberg C, Kissmeyer AM, Latini S, Mathiasen IS and Mørk Hansen C, The need for new vitamin D analogues: Mechanisms of action and clinical applications. In: *Vitamin D, A Pluripotent Steroid Hormone: Structural Studies, Molecular Endocrinology and Clinical Applications, Proceedings on the Ninth Workshop on Vitamin D, Florida, USA, 28 May–2 June 1994*. (Eds. Norman AW, Bouillon R and Thomasset M), pp. 55–63. Walter de Gruyter, New York, 1994.
17. Binderup L and Bramm E, Effects of a novel vitamin D analogue MC 903 on cell proliferation and differentiation *in vitro* and on calcium metabolism *in vivo*. *Biochem Pharmacol* **37:** 889–895, 1988.
18. Guo Y-D, Strugnell S, Back DW and Jones G, Transfected human liver cytochrome P-450 hydroxylates vitamin D analogs at different side-chain positions. *Proc Natl Acad Sci* **90:** 8668–8672, 1993.
19. Tanaka Y, Schnoes HK, Smith CM and Deluca HF, 1,25,26-Trihydroxyvitamin D_3: Isolation, identification and biological activity. *Arch Biochem Biophys* **210:** 104–109, 1981.
20. Reinhardt TA, Napoli JL, Beitz DC, Littledike ET and Horst RL, A new *in vivo* metabolite of vitamin D_3: 1,25,26-trihydroxyvitamin D_3. *Biochem Biophys Res Commun* **99:** 302–307, 1981.
21. Horst RL, Wovkulich PM, Baggiolini EG, Uskokovic MR, Engstrom GW and Napoli JL, (23S)-1,23,25-Trihydroxyvitamin D_3: Its biological activity and role in 1α,25-dihydroxyvitamin D_3 26,23-lactone biosynthesis. *Biochemistry* **23:** 3973–3979, 1984.

22. Patel SR, Ke HQ and Hsu CH, Effect of vitamin D metabolites on calcitriol degradative enzymes in renal failure. *Kidney Int* **45:** 509–514, 1994.
23. Roy S, Martel J and Tenenhouse HS, Comparative effects of 1,25-dihydroxyvitamin D_3 and EB 1089 on mouse renal and intestinal 25-hydroxyvitamin D_3-24-hydroxylase. *J Bone Miner Res* **10:** 1951–1959, 1995.
24. Masuda S, Byford V, Kremer R, Makin HLJ, Kubodera N, Nishii Y, Okazaki A, Okano T, Kobayashi T and Jones G, *In vitro* metabolism of a vitamin D analog 22-oxacalcitriol using cultured osteosarcoma, hepatoma and keratinocyte cell lines. *J Biol Chem* **271:** 8700–8708, 1996.
25. Brown AJ, Berkoben M, Ritter C, Kubodera N, Nishii Y and Slatopolsky E, Metabolism of 22-oxacalcitriol by a vitamin D-inducible pathway in cultured parathyroid cells. *Biochem Biophys Res Commun* **189:** 759–764, 1992.
26. Grieff M, Dusso A, Mori T, Nishii Y, Slatopolsky E and Brown AJ, 22-Oxacalcitriol suppresses 25-hydroxycholecalciferol-1α-hydroxylases in rat kidney. *Biochem Biophys Res Commun* **185:** 191–196, 1992.
27. Mørk Hansen C, Mathiasen IS, Binderup L, The antiproliferative and differentiation-inducing effects of vitamin D analogs are not determined by the binding affinity for the vitamin D receptor alone. *J Invest Dermatol Symp Proc* **1:** 44–48, 1995.